OMTN, Volume *10*

Supplemental Information

RNA Nanotherapeutics for the Amelioration of Astroglial Reactivity

Jayden A. Smith, Alice Braga, Jeroen Verheyen, Silvia Basilico, Sara Bandiera, Clara Alfaro-Cervello, Luca Peruzzotti-Jametti, Dan Shu, Farzin Haque, Peixuan Guo, and Stefano Pluchino

Supplemental Information

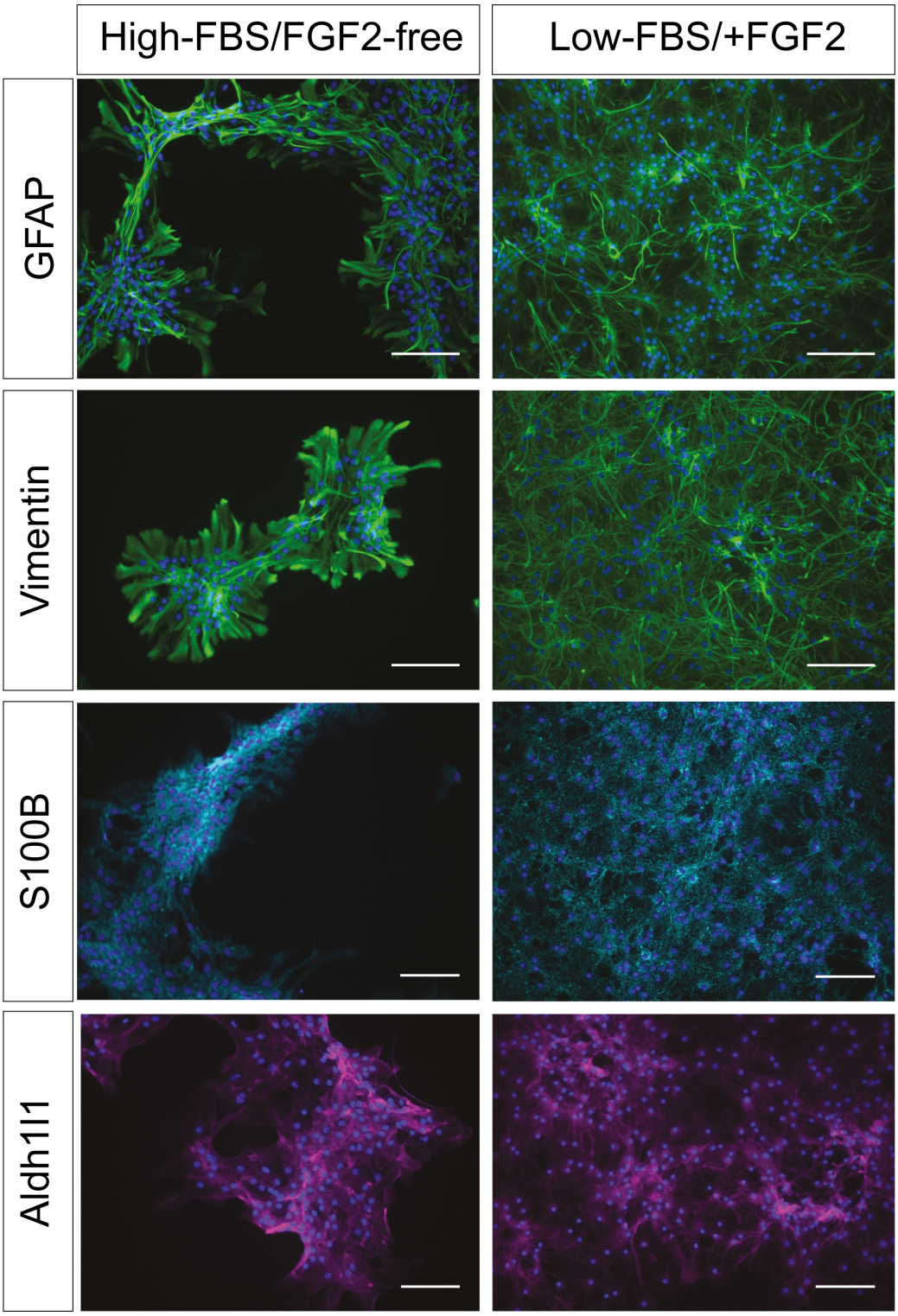

Figure S1. Immunofluorescence characterisation of high-FBS/FGF2-free versus low-FBS/+FGF2 cultured astrocytes. From top-to-bottom, comparative morphology and expression of astroglial markers GFAP, Vimentin, S100B, and Aldh1l1 in high-FBS/FGF2-free (left column) and low-FBS/+FGF2 (right column) cultured astrocytes. Nuclei counterstained with DAPI (blue). Scale bar = 100 μm.

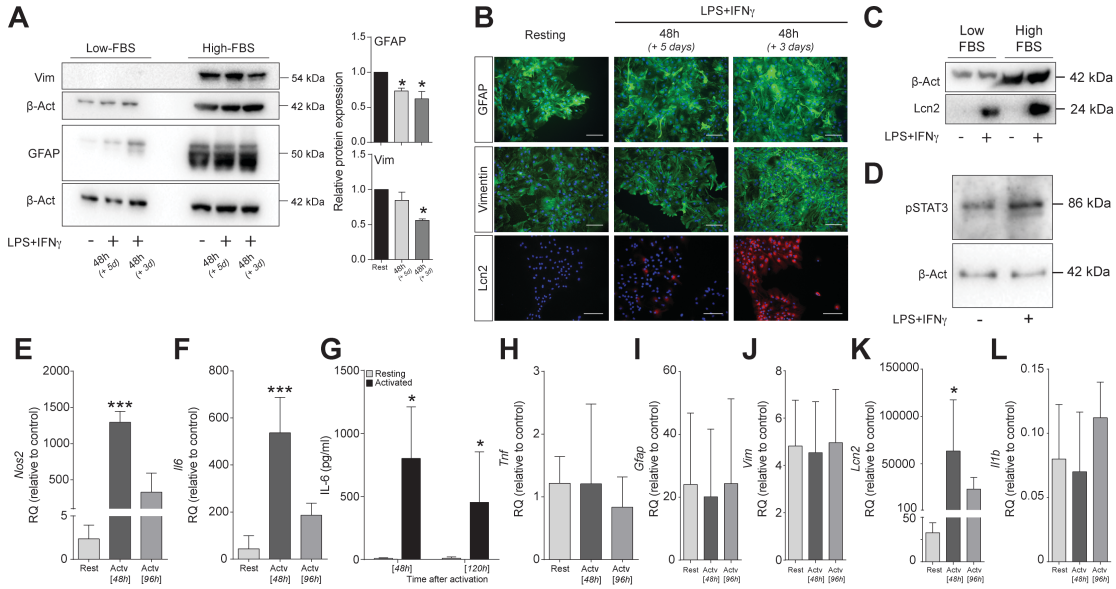

Figure S2. Response of high-FBS/FGF2-free cultured astrocytes to LPS+IFN-γ stimulation. (A) Representative Western blots showing GFAP and Vim protein expression levels 3 and 5 days after a 48h activation period, as compared to comparative conditions in low-FBS astrocytes. Densitometric quantification of GFAP and Vim Western blot expression relative to β-actin, normalised to resting conditions, is depicted alongside. **(B)** Immunofluorescence micrographs of resting and activated high-FBS/FGF2-free astrocytes showing expression of GFAP, Vim and Lcn2. Activated astrocytes imaged 3 and 5 days after a 48h activation period (GFAP/Vim: green, DAPI-stained nuclei: blue). **(C)** Representative Western blot showing expression of Lcn2 (23 kDa) upon 24h of LPS+IFN-γ exposure, in low- and high-FBS conditions. (**D**) pSTAT3 (Tyr705) in resting and activated (1h LPS+IFN-γ stimulation) high-FBS/FGF2-free astrocytes. **(E, F** and **H-K)**: qPCR quantification of **(E)** *Nos2*, **(F)** *Il6*, and **(H)** *Tnf*, **(H)** *Il6,* **(I)** *Gfap*, **(J)** *Vim*, **(K)** *Lcn2*, and **(L)** *Il1b* levels in resting and LPS+IFN-γ-treated high-FBS astrocytes (48 and 96 hours after activation). Expression relative to resting low-FBS/+FGF2 controls ($2^{-\Delta\Delta Ct}$ method), *Gapdh* reference gene. **(G)** Secreted IL-6 as measured by ELISA, resting *vs*. activated conditions, at 48h and 120h post-stimulation. All data expressed as the mean of n≥ 3 biological replicates ± SD; * p≤ 0.05, ** p≤ 0.01, *** p≤ 0.001, or **** p≤ 0.0001 relative to non-activated control samples (qPCR and Western blot: one-way ANOVA with Dunnett's multiple comparison test; ELISA: multiple t-tests with statistical significance determined using the Holm-Sidak method, α= 0.05).

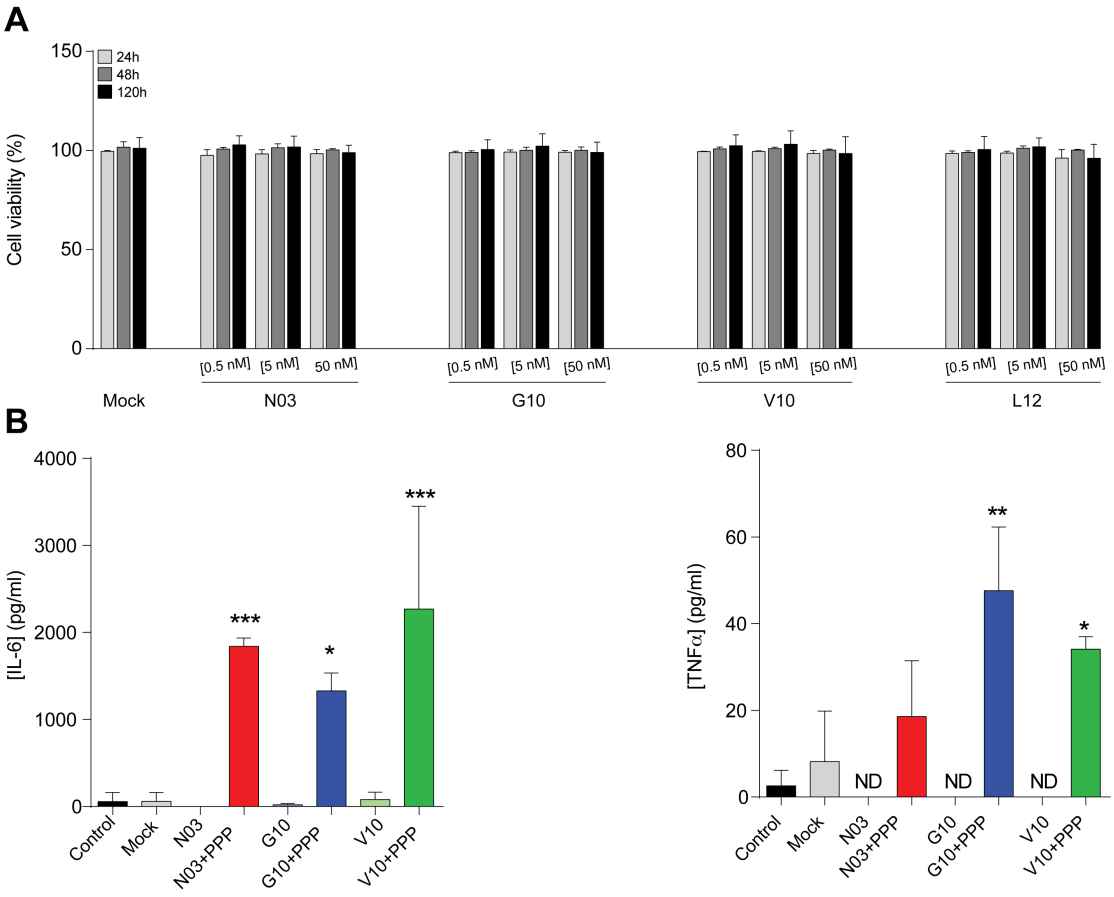

Figure S3. Dephosphorylated siRNA-3WJ nanostructures do not induce pro-inflammatory secretions and are non-toxic. (**A**) LDH cytotoxicity assay comparing the effect of 0.5, 5, and 50 nM doses of the siRNA-3WJ nanostructures employed in this study in low-FBS astrocytes. Supernatant LDH levels were determined colorimetrically at 24h, 48h and 120h after transfection, with a calibration establishing non-treated cells as 100% viable, lysed cells as 0% viable. N = 3 biological replicates, ± SD, with no statistically significant differences between treatments. (**B**) Quantification of IL-6 and TNF-α concentrations (pg/ml) in the supernatant of astrocytes treated with 3WJs with (+PPP) or without 5′-triphosphate groups. Results expressed as the mean cytokine concentration measured from n≥ 2 biological replicates ± SD; * p≤ 0.05, ** p≤ 0.01, *** p≤ 0.001, or **** p≤ 0.0001 relative to untreated control samples (one-way ANOVA with Dunnett's multiple comparison test); ND = Not Determined.

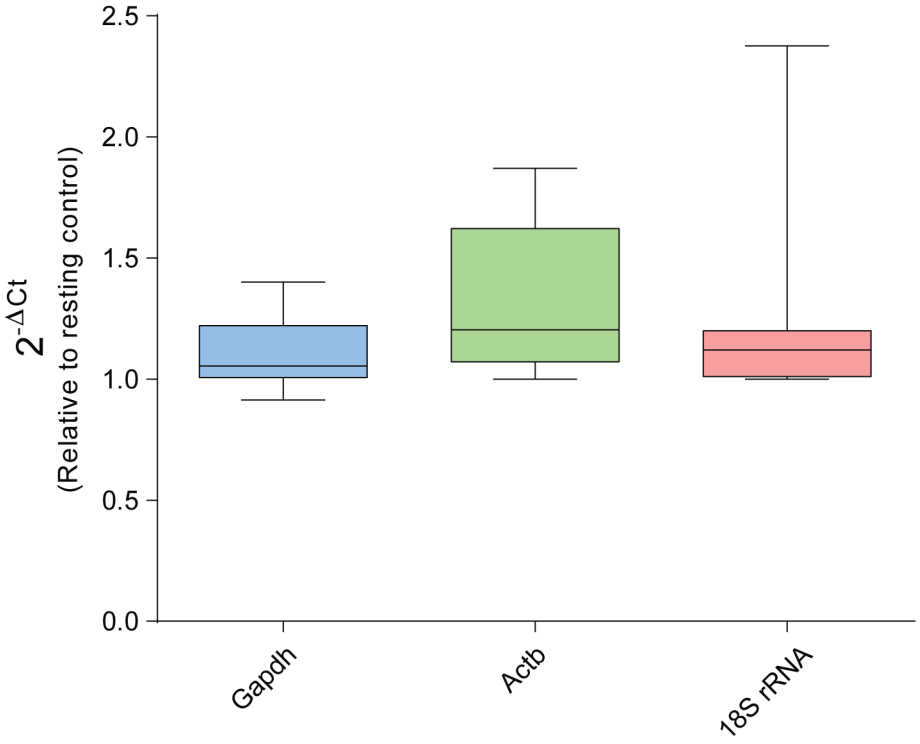

Figure S4. Reference gene expression remains stable across treatment and activation conditions. The stability of the putative genes of reference *Gapdh*, *Actb*, and *RNa18s5* were assayed across control, mock and N03-3WJ transfected treatments, under resting and both *Therapeutic* and *Preventative* activation profiles. Data are expressed as $2^{-\Delta Ct}$, where ΔCt is the mean difference in qPCR cycle threshold numbers of the reference gene between the resting control and treated sample. Results expressed as a box-and-whiskers plot of n≥ 3 biological replicates, with the box spanning the 25^{th} to 75^{th} percentiles and the whiskers spanning the min and max values. No statistical significance observed between reference genes.

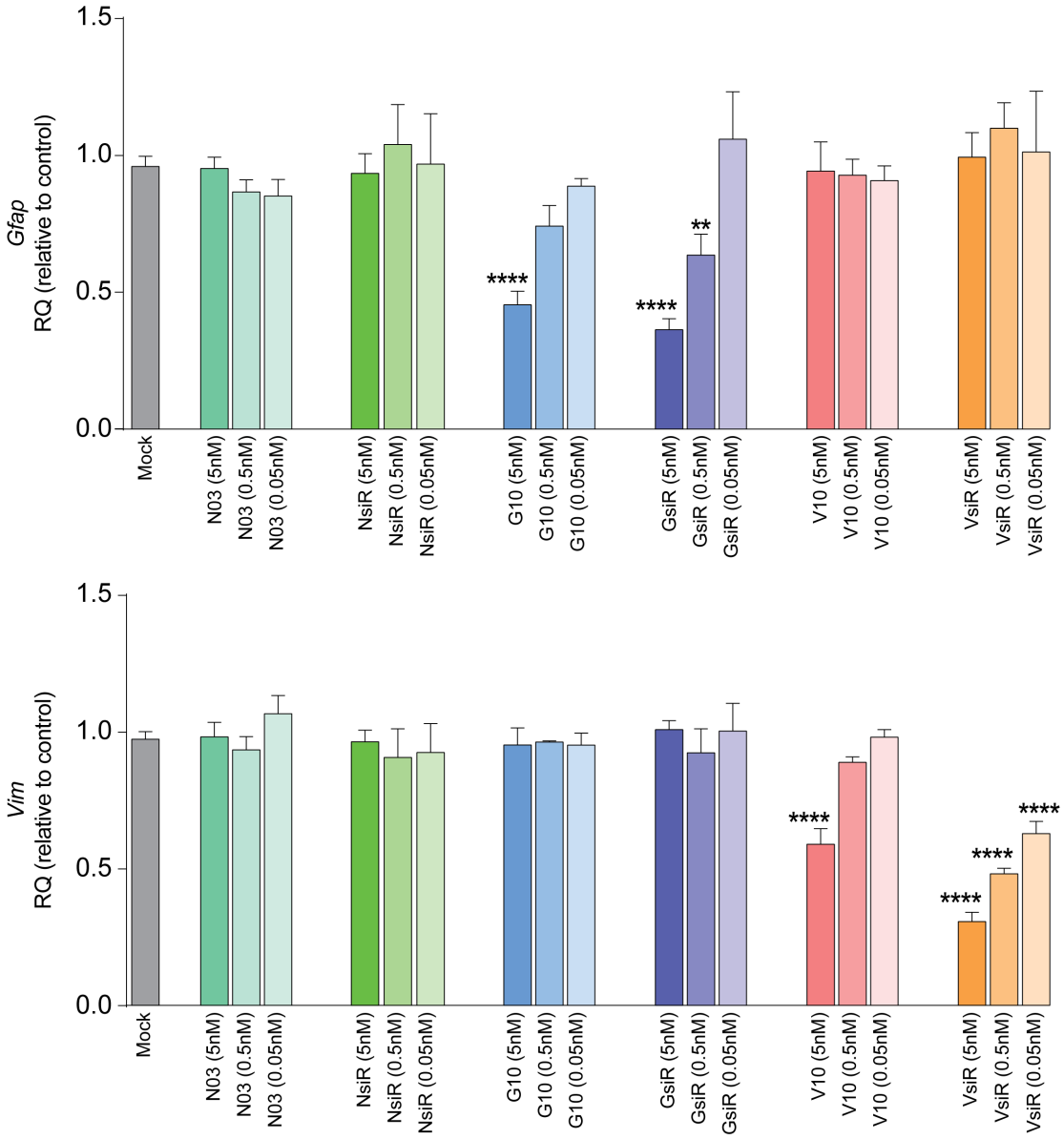

Figure S5. 3WJs knock down the expression of intermediate filament genes in a dose-responsive manner with efficiencies similar to commercial siRNA pools. (A) *Gfap* and **(B)** *Vim* mRNA knockdown measured in high-FBS/FGF-free matured astrocytes under resting conditions upon Lipofectamine RNAiMAX-mediated transfection. Non-targeted, anti-*Gfap* and anti-*Vim* 3WJs (N03, G10 and V10, respectively) are compared to analogous siRNA pools (NsiR, GsiR and VsiR, respectively). Results are expressed as the mean mRNA expression (qPCR) of n≥ 6 biological replicates ± SD; *Gapdh* reference gene; * p≤ 0.05, ** p≤ 0.01, *** p≤ 0.001, or **** p≤ 0.0001 relative to control samples (one-way ANOVA with Dunnett's multiple comparison test).

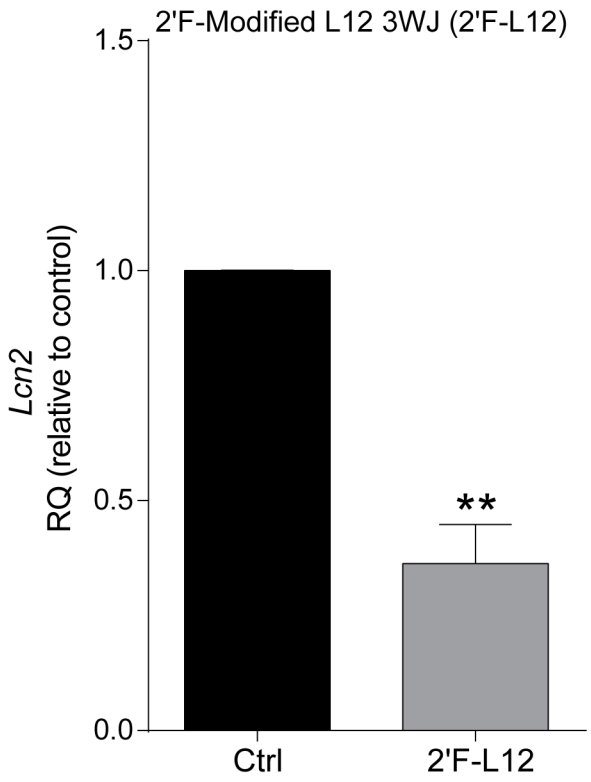

Figure S6. *In vitro* knockdown of *Lcn2* mRNA by 2'-fluoro modified L12-3WJ. qPCR data showing significant downregulation of Lcn2 mRNA by a lipofected 5 nM dose of 2'F-L12-3WJ as compared to non-treated astrocytes. Astrocytes activated with LPS+IFN-γ treatment (*Preventative* conditions), mRNA expression measure 48h after transfection. *Gapdh* reference gene. Data expressed as the mean RQ of n= 3 biological replicates ± SD; ** p≤ 0.01 relative to non-treated samples (unpaired t-test with Welch's correction).

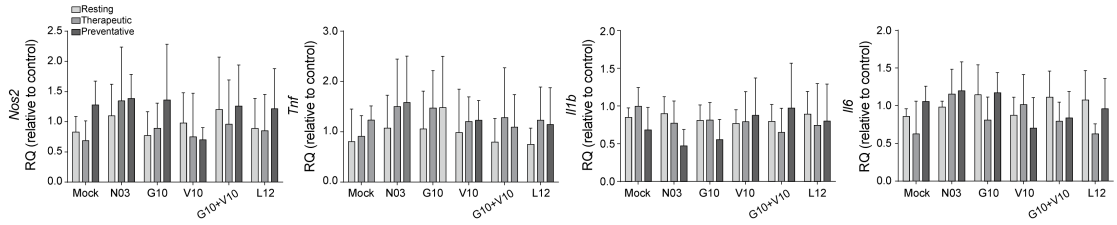

Figure S7. Neither 3WJ transfection nor knockdown of *Gfap*, *Vim* or *Lcn2* affects the expression of pro-inflammatory markers under resting or activated conditions. mRNA levels of several pro-inflammatory markers known to be upregulated in reactive low-FBS astrocytes: *Nos2*, *Tnf*, *Il1b* and *Il6*. Results are expressed as the mean mRNA expression (qPCR) of n≥ 2 biological replicates ± SD; *Gapdh* reference gene; * p≤ 0.05, ** p≤ 0.01, *** p≤ 0.001, or **** p≤ 0.0001 relative to control samples of the same activation state (two-way ANOVA with Dunnett's multiple comparison test).

Table S1. siRNA moieties of pRNA 3WJ nanostructures used in this work.

3WJ	Target	Analogous ON-TARGET siRNA[a]	Target (Sense) Sequence
G10	*Gfap* (mouse)	J-043455-10	AGC ACG AAG CUA ACG ACU A
V10	*Vim* (mouse)	J-061596-10	AGG AAG AGA UGG CUC GUC A
L12	*Lcn2* (mouse)	J-042638-12	GCG CAG AGA CCC AAU GGU U
N03	Non-Targeting	D-001810-03	UGG UUU ACA UGU UUU CUG A

[a]Individual siRNA components of the L-043455-01 anti-GFAP, L-061596-01 anti-Vim, L-042638-01 or D-001810-10 non-targeting ON-TARGET SMARTpools, as appropriate.

Table S2. Primary and secondary antibodies used in in this work.

Antibody	Supplier	Dilution
Chicken anti-GFAP	Abcam (ab4674)	1:500
Rabbit anti-GFAP	Dako (Z0334)	1:500
Chicken anti-Vimentin	Abcam (ab73159)	1:500
Rat anti-Lipocalin2	R&D Systems (MAB1857)	1:250
Mouse anti-S100B	BD Bioscience (BD612376)	1:500
Rabbit anti-Aldh1l1	Abcam (AB87117)	1:250
Rabbit anti-pSTAT3	Cell Signaling (9145)	1:100
AlexaFluor488 anti-chicken	Invitrogen	1:1,000
AlexaFluor488 anti-rabbit	Invitrogen	1:1,000
AlexaFluor546 anti-mouse	Invitrogen	1:1,000
AlexaFluor546 anti-rabbit	Invitrogen	1:1,000
AlexaFluor647 anti-rabbit	Invitrogen	1:1,000

Table S3. TaqMan Gene Expression Assay reagents used in this work.

Target Gene	TaqMan Assay
Gfap	Mm01253033_m1
Vim	Mm01333430_m1
Lcn2	Mm01324470_m1
Nes	Mm00450205_m1
Il6	Mm00446190_m1
Tnf	Mm00443258_m1
Ifnb1	Mm00439552_s1
Nos2	Mm00440502_m1
Ciita	Mm00482914_m1
Il1b	Mm00434228_m1
Tlr4	Mm00445273_m1
Ifngr1	Mm00599890_m1
Ifngr2	Mm00492626_m1
Gapd	4352339E
Actb	4319413E
18s	4352341E

Table S4. Primary antibodies used in this work.

Antibody	Supplier	Dilution
Rabbit anti-GFAP	Dako (Z0334)	1:10,000
Mouse anti-Vimentin	Abcam (ab8978)	1:500
Rat anti-Lipocalin 2	R&D Systems (MAB1857)	1:1,000
Rabbit anti-pSTAT3 (Tyr705)	Cell Signaling (9145)	1:1,000
Mouse anti-β-actin	Sigma (A1978)	1:10,000